proceedings

MDPI

Proceedings

Effects of Guanidinium and Formamidinium Addition to $CH_3NH_3PbI_3$-Based Perovskite Solar Cells †

Taku Kishimoto, Atsushi Suzuki, Naoki Ueoka and Takeo Oku *

Department of Materials Science, The University of Shiga Prefecture, 2500 Hassaka, Hikone, Shiga 522-8533, Japan; oi21tkishimoto@ec.usp.ac.jp (T.K.); suzuki@mat.usp.ac.jp (A.S.); oh21nueoka@ec.usp.ac.jp (N.U.)

* Correspondence: oku@mat.usp.ac.jp; Tel.: +81-749-28-8368

† Presented at the 2nd International Online-Conference on Nanomaterials, 15–30 November 2020; Available online: https://iocn2020.sciforum.net/.

Published: 15 November 2020

Abstract: Additive effects of guanidinium [$C(NH_2)_3$, GA] iodide, formamidinium [$CH(NH_2)_2$, FA] iodide, and guanidinium chloride to $CH_3NH_3PbI_3$-based photovoltaic devices were investigated. Short-circuit current densities, open-circuit voltages, series resistances and shunt resistances were improved by the GA addition. The short-circuit current densities were increased by FA addition with GA, and the external quantum efficiencies increased, which resulted in suppression of pin-holes in perovskite layers by the GA addition. X-ray diffraction showed that the lattice constants of the perovskite crystals increased by the GA and FA addition, and that the GA substituted partially at the CH_3NH_3-site.

Keywords: perovskite; solar cell; photovoltaic device; guanidinium; formamidinium

1. Introduction

Recently, thin film solar cells with perovskite-type methylammonium trihalogenoplumbates (II) ($CH_3NH_3PbI_3$) compounds have been widely studied due to their easy fabrication processes and high conversion efficiencies compared to conventional organic solar cells [1–4]. It has been reported that the photovoltaic properties of perovskite solar cells depended severely on the compositions and crystal structures of the perovskite compounds. Doping with such elements as cesium [5], rubidium [6,7], potassium [8–10], sodium [11], formamidinium ($CH(NH_2)_2$, FA) [10,12], ethylammonium ($CH_3CH_2NH_3$, EA) [13], or guanidinium ($C(NH_2)_3$, GA) [14–16] at the methylammonium (CH_3NH_3, MA) sites improved the conversion efficiencies. Studies on doping with halogen atoms, such as chlorine (Cl) [17–23] or bromine (Br) [6], at the iodine (I) sites of the perovskite crystals have also been reported. The doped Cl ions were found to lengthen the diffusion length of excitons, which resulted in improvement of the conversion efficiency [17,19]. Various elemental substituted perovskite compounds have been reported [24].

The purpose of the present work was to investigate the effects of GAI, GACl and FAI addition to $CH_3NH_3PbI_{3-x}Cl_x$-based perovskite [16]. The GA addition is expected to extend the carrier life time and to reduce the carrier recombination in the perovskite layers [15]. The GACl addition is expected to provide effects of both GA and Cl additions. FA addition is also expected to expand the wavelength range of light adsorption [4]. The effects of these additives on the formation of perovskite compounds for the photovoltaic cells were investigated by light-induced current density-voltage (J-V) characteristics, incident photon-to-current conversion efficiency (IPCE), X-ray diffraction (XRD), optical microscopy, and scanning electron microscopy (SEM) with energy dispersive X-ray spectrometry (EDS).

2. Experimental

Details of the basic fabrication process are described in published reports [24–27]. F-doped tin oxide (FTO) substrates were cleaned using an ultrasonic bath with acetone and methanol, and dried under nitrogen gas. 0.15 and 0.30 M TiO_2 precursor solutions were prepared from titanium diisopropoxide bis(acetylacetonate) (Sigma-Aldrich, 0.055 and 0.11 mL) with 1-butanol (1 mL), and the 0.15 M TiO_2 precursor solution was spin-coated on the FTO substrate at 3000 rpm for 30 s and heated at 125 °C for 5 min in air to form a TiO_x layer. The 0.30 M TiO_2 precursor solution was spin-coated onto the TiO_x layer at 3000 rpm for 30 s, and heated at 125 °C for 5 min. This process of coating with a 0.30 M solution was then performed two times, and the FTO substrate was annealed at 550 °C for 30 min to form a compact TiO_2 layer. For the mesoporous TiO_2 layer, TiO_2 paste was prepared with TiO_2 powder (Nippon Aerosil, P-25) with poly(ethylene glycol) (Nacalai Tesque, PEG #20000) in ultrapure water. The solution was mixed with acetylacetone (Wako Pure Chemical Industries, 10 μL) and triton X-100 (Sigma-Aldrich, 5 μL) for 30 min, and then left for 12 h to suppress the bubbles in the solution. After that, the TiO_2 paste was coated onto the substrate by spin-coating at 5000 rpm for 30 s. The cells were then annealed at 120 °C for 5 min and at 550 °C for 30 min to form a mesoporous TiO_2 layer.

For the preparation of perovskite compounds, a solution of CH_3NH_3I (Showa Chemical Co. Ltd. (Tokyo, Japan), 190.7 mg) and $PbCl_2$ (Sigma-Aldrich (St. Louis, MO, USA), 111.2 mg) was prepared with a mole ratio of 3:1 and in N,N-dimethylformamide (Nacalai Tesque, 500 μL) with additives of GAI (10 mol%, 7.5 mg), GACl (10 mol%, 3.8 mg), and GAI + FAI (10 mol%, 7.5 and 6.9 mg). These perovskite cells are denoted +GAI, +GACl, and +GAI+FACl, respectively. The reaction mechanism proposed for the $CH_3NH_3PbI_3$ perovskite is as follows: $3CH_3NH_3I + PbCl_2 \rightarrow CH_3NH_3PbI_3 + 2CH_3NH_3Cl(\uparrow)$. Since $2CH_3NH_3Cl$ is generated as a byproduct during the reaction, the quantity 10 mol% means 10 mol% of the produced $CH_3NH_3PbI_3$. The solutions were stirred at 70 °C for 24 h. Then, the solutions of $CH_3NH_3PbI_3(Cl)$ were introduced into the TiO_2 mesopores by the spin-coating method and annealed at 150 °C for 20 min (perovskite with additive) or 140 °C for 15 min (standard) to form the perovskite layer. A hole transport layer was then prepared by spin-coating onto the perovskite layer. For the hole transport layer, a chlorobenzene solution of 0.5 mL was mixed with a solution of lithium bis(trifluoromethylsulfonyl)imide (Li-TFSI, Tokyo Chemical Industry (Tokyo, Japan), 260 mg) in acetonitrile (Nacalai Tesque (Singapore City, Singapore), 0.5 mL) for 12 h. The former solution with 4-tert-butylpyridine (Aldrich, 14.4 μL) was mixed with the Li-TFSI solution (8.8 μL) for 30 min at 70 °C. All procedures for preparation of the thin contacts were evaporated as top metal electrodes. The layered structures of the present solar cells were denoted FTO/TiO_2/perovskite/spiro-OMeTAD/Au, as shown in Figure 1. The *J-V* characteristics of the photovoltaic cells were measured under illumination at 100 mW cm^{-2} using an AM 1.5 solar simulator (San-ei Electric, XES-301S, Osaka, Japan).

The *J-V* measurements were performed by source measure unit (Keysight, B2901A Precision SMU). The scan rate and sampling time were ~0.08 V s^{-1} and 1 ms, respectively. Four cells were tested for each condition. The solar cells were illuminated through the sides of the FTO substrates, and the illuminated area was 0.090 cm^2. The IPCE of the cells were also measured (Enli Technology, QE-R). The microstructures of the present cells were investigated using an X-ray diffractometer (Bruker, D2 PHASER), a transmission optical microscope (Nikon, Eclipse E600) and a scanning electron microscope (Jeol, JSM-6010PLUS/LA) equipped with EDS.

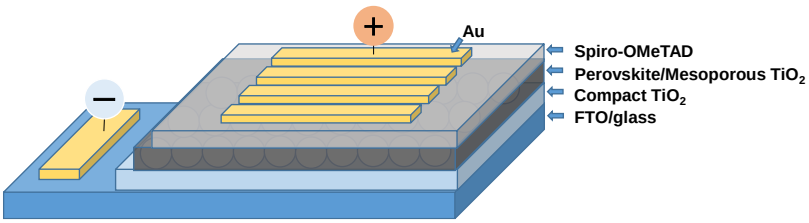

Figure 1. Layered structure of the present solar cells (FTO/TiO_2/perovskite/spiro-OMeTAD/Au).

3. Results and Discussion

Figure 2 shows the *J-V* characteristics of the TiO_2/ perovskite/spiro-OMeTAD photovoltaic cells under illumination, which indicates the effects of the GA and FA addition [16]. The measured photovoltaic parameters of the cells are summarized in Table 1. Standard $CH_3NH_3PbI_3$(Cl) cells provided a power conversion efficiency (η) of 5.31%, and the averaged efficiency (η_{ave}) of four electrodes on the cells is 4.42%, as listed in Table 1. The short-circuit current density (J_{SC}), open-circuit voltage (V_{OC}) and fill factor (FF) were increased by GAI addition and the highest efficiency 12.51% was obtained for the +GAI cell. The highest J_{SC} and V_{OC} were obtained for +GAI+FAI cells, which provided an η of 11.66% and η_{ave} of 11.01%. FF values of the +GAI+FAI cells were lower than that of +GAI cells. Addition of GACl to $CH_3NH_3PbI_3$(Cl) provided a higher η of 9.14% than that of the standard cells, but lower than that of +GAI cells. Table 1 shows that the series resistances (R_S) and the shunt resistances (R_{Sh}) were decreased and increased by the GA addition, respectively. These results lead to the improvements of J_{SC} and V_{OC}. Further improvements could be expected by optimizing the compositions and annealing conditions.

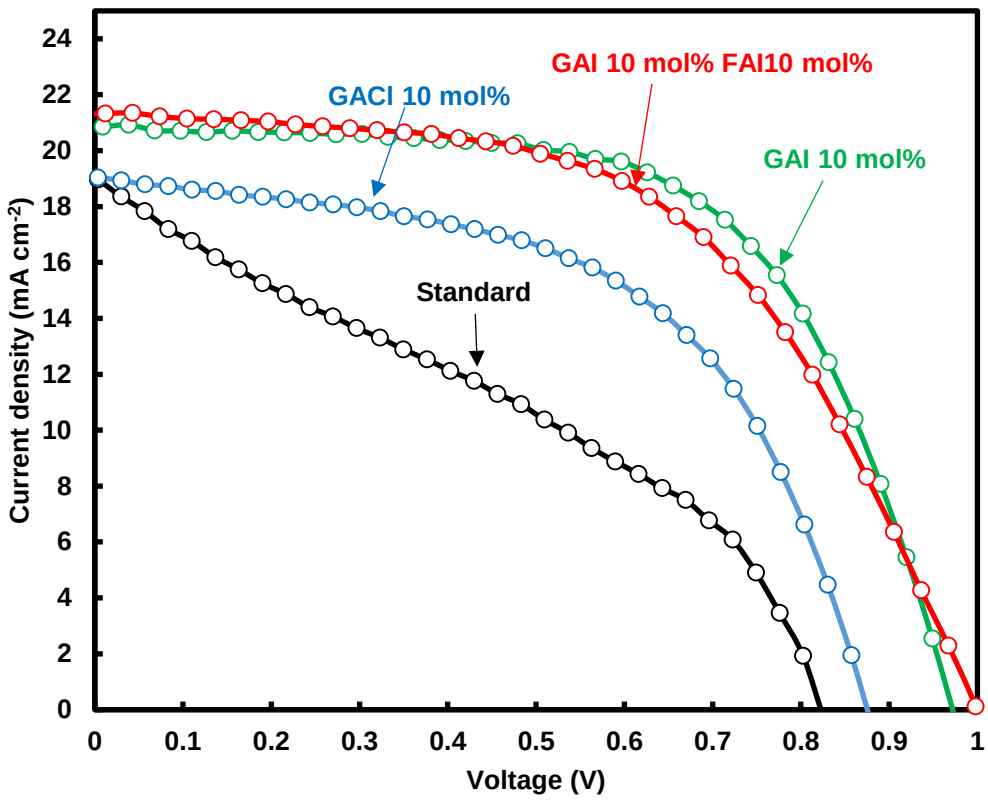

Figure 2. *J-V* characteristics of the present perovskite photovoltaic cells.

Table 1. Measured photovoltaic parameters of solar cells.

Device	J_{SC} (mA cm^{-2})	V_{OC} (V)	FF	η (%)	η_{ave} (%)	R_S (Ω cm^2)	R_{Sh} (Ω cm^2)	E_g (eV)
Standard	19.0	0.823	0.339	5.31	4.42	9.64	70	1.55
+GAI	20.9	0.972	0.616	12.51	11.20	7.05	1599	1.53
+GACl	19.1	0.875	0.548	9.14	7.30	8.20	290	1.53
+GAI+FAI	21.3	0.999	0.547	11.66	11.01	8.92	667	1.54

4. Conclusions

Photovoltaic properties such as J_{SC}, V_{OC}, R_S and R_{Sh} of $MAPbI_{3-x}Cl_x$-based perovskite photovoltaic cells were improved by GA addition. Increase of J_{SC} and V_{OC} by the GA and FA addition implies that MA-GA-FA mixed cation based perovskite solar cells have a potential for further improvement of the photovoltaic performances.

Author Contributions: Conceptualization, T.K. A.S. and T.O.; Methodology, T.K., N.U., and A.S.; Formal Analysis, T.K. and T.O.; Investigation, T.K.; Data Curation, T.K. and T.O.; Writing-Original Draft Preparation, T.K. and T.O.; Writing-Review & Editing, T.O.; Visualization, T.K. and T.O.; Supervision, A.S. and T.O.; Project Administration, T.O.; Funding Acquisition, T.O. All authors have read and agreed to the published version of the manuscript.

Funding: This research was partly funded by the Super Cluster Program of the Japan Science and Technology Agency (JST).

Conflicts of Interest: The authors declare no conflict of interest.

References

1. Kojima, A.; Teshima, K.; Shirai, Y.; Miyasaka, T. Organometal halide perovskites as visible-light sensitizers for photovoltaic cells. *J. Am. Chem. Soc.* **2009**, *131*, 6050–6051, doi:10.1021/ja809598r.
2. Kim, H.-S.; Lee, C.-R.; Im, J.-H.; Lee, K.-B.; Moehl, T.; Marchioro, A.; Moon, S.-J.; Yum, J.-H.; Humphry-Baker, R.; Moser, J.E.; et al. Lead iodide perovskite sensitized all-solid-state submicron thin film mesoscopic solar cell with efficiency exceeding 9%. *Sci. Rep.* **2012**, *2*, 591, doi:10.1038/srep00591.
3. Lee, M.M.; Teuscher, J.; Miyasaka, T.; Murakami, T.N.; Snaith, H.J. Efficient hybrid solar cells based on meso-superstructured organometal halide perovskites. *Science* **2012**, *338*, 643–647, doi:10.1126/science.1228604.
4. Yang, W.S.; Noh, J.H.; Jeon, N.J.; Kim, Y.C.; Ryu, S.; Seo, J.; Seok, S.I. High-performance photovoltaic perovskite layers fabricated through intramolecular exchange. *Science* **2015**, *348*, 1234–1237, doi:10.1126/science.aaa9272.
5. Saliba, M.; Matsui, T.; Seo, J.Y.; Domanski, K.; Correa-Baena, J.P.; Nazeeruddin, M.K.; Zakeeruddin, S.M.; Tress, W.; Abate, A.; Hagfeldtd, A.; et al. Cesium-containing triple cation perovskite solar cells: Improved stability, reproducibility and high efficiency. *Energy Environ. Sci.* **2016**, *9*, 1989–1997, doi:10.1039/C5EE03874J.
6. Saliba, M.; Matsui, T.; Domanski, K.; Seo, J.Y.; Ummadisingu, A.; Zakeeruddin, S.M.; Baena, J.P.C.; Tress, W.R.; Abate, A.; Hagfeldt, A.; et al. Incorporation of rubidium cations into perovskite solar cells improves photovoltaic performance. *Science* **2016**, *354*, 206–209, doi:10.1126/science.aah5557.
7. Ueoka, N.; Oku, T.; Suzuki, A. Additive effects of alkali metals on Cu-modified $CH_3NH_3PbI_{3-\delta}Cl_\delta$ photovoltaic devices. *RSC Adv.* **2019**, *9*, 24231–24240.
8. Machiba, H.; Oku, T.; Kishimoto, T.; Ueoka, N.; Suzuki, A. Fabrication and evaluation of K-doped $MA_{0.8}FA_{0.1}K_{0.1}PbI_3$(Cl) perovskite solar cells. *Chem. Phys. Lett.* **2019**, *730*, 117–123.
9. Kandori, S.; Oku, T.; Nishi, K.; Kishimoto, T.; Ueoka, N.; Suzuki, A. Fabrication and characterization of potassium- and formamidinium-added perovskite solar cells. *J. Ceram. Soc. Jpn.* **2020**, *128*, 805–811, doi:10.2109/jcersj2.20090.
10. Oku, T.; Kandori, S.; Taguchi, M.; Suzuki, A.; Okita, M.; Minami, S.; Fukunishi, S.; Tachikawa, T., Polysilane-inserted methylammonium lead iodide perovskite solar cells doped with formamidinium and potassium. *Energies* **2020**, *13*, 4776−1−12, doi:10.3390/en13184776.
11. Ueoka, N.; Oku, T. Effects of co-addition of sodium chloride and copper(II) bromide to mixed-cation mixed-halide perovskite photovoltaic devices. *ACS Appl. Energy Mater.* **2020**, *3*, 7272–7283, doi:10.1021/acsaem.0c00182.
12. Suzuki, A.; Kato, M.; Ueoka, N.; Oku, T. Additive effect of formamidinium chloride in methylammonium lead halide compound-based perovskite solar cells. *J. Electron. Mater.* **2019**, *48*, 3900−3907, doi:10.1007/s11664-019-07153-2.
13. Nishi, K.; Oku, T.; Kishimoto, T.; Ueoka, N.; Suzuki, A. Photovoltaic characteristics of $CH_3NH_3PbI_3$ perovskite solar cells added with ethylammonium bromide and formamidinium iodide. *Coatings* **2020**, *10*, 410−1−10, doi:10.3390/coatings10040410.

14. Hou, X.; Hu, Y.; Liu, H.; Mei, A.; Li, X.; Duan, M.; Zhang, G.; Rong, Y.; Han, H. Effect of guanidinium on mesoscopic perovskite solar cells. *J. Mater. Chem. A* **2017**, *5*, 73–78, doi:10.1039/C6TA08418D.
15. Jodlowski, A.D.; Roldán-Carmona, C.; Grancini, G.; Salado, M.; Ralaiarisoa, M.; Ahmad, S.; Koch, N.; Camacho, L.; Miguel, G.; Nazeeruddin, M. Large guanidinium cation mixed with methylammonium in lead iodide perovskites for 19% efficient solar cells. *Nat. Energy* **2017**, *2*, 972–979, doi:10.1038/s41560-017-0054-3.
16. Kishimoto, T.; Suzuki, A.; Ueoka, N.; Oku, T. Effects of guanidinium addition to $CH_3NH_3PbI_{3-x}Cl_x$ perovskite photovoltaic devices. *J. Ceram. Soc. Jpn.* **2019**, *127*, 491–497, doi:10.2109/jcersj2.18214.
17. Stranks, S.D.; Eperon, G.E.; Grancini, G.; Menelaou, C.; Alcocer, M.J.P.; Leijtens, T.; Herz, L.M.; Petrozza, A.; Snaith, H.J. Electron-hole diffusion lengths exceeding 1 micrometer in an organometal trihalide perovskite absorber. *Science* **2013**, *342*, 341–344, doi:10.1126/science.1243982.
18. Shi, D.; Adinolfi, V.; Comin, R.; Yuan, M.; Alarousu, E.; Buin, A.; Chen, Y.; Hoogland, S.; Rothenberger, A.; Katsiev, K.; et al. Low trap-state density and long carrier diffusion in organolead trihalide perovskite single crystals. *Science* **2015**, *347*, 519–522, doi:10.1126/science.aaa2725.
19. Dong, Q.; Fang, Y.; Shao, Y.; Mulligan, P.; Qiu, J.; Cao, L.; Huang, J. Electron-hole diffusion lengths > 175 μm in solution-grown $CH_3NH_3PbI_3$ single crystals. *Science* **2015**, *347*, 967–970, doi:10.1126/science.aaa5760.
20. Oku, T.; Suzuki, K.; Suzuki, A. Effects of chlorine addition to perovskite-type $CH_3NH_3PbI_3$ photovoltaic devices, *J. Ceram. Soc. Jpn.* **2016**, *124*, 234–238, doi:10.2109/jcersj2.15250.
21. McLeod, J.A.; Wu, Z.; Sun, B.; Liu, L. The influence of the I/Cl ratio on the performance of $CH_3NH_3PbI_{3-x}Cl_x$-based solar cells: Why is $CH_3NH_3I : PbCl_2$ = 3 : 1 the "magic" ratio? *Nanoscale* **2016**, *8*, 6361–6368, doi:10.1039/C5NR06217A.
22. Oku, T.; Ohishi, Y.; Suzuki, A.; Miyazawa, Y. Effects of NH_4Cl addition to perovskite $CH_3NH_3PbI_3$ photovoltaic devices. *J. Ceram. Soc. Jpn*. **2017**, *125*, 303–307, doi:10.2109/jcersj2.16279.
23. Oku, T.; Ohishi, Y. Effects of annealing on $CH_3NH_3PbI_3$(Cl) perovskite photovoltaic devices. *J. Ceram. Soc. Jpn.* **2018**, *126*, 56–60, doi:10.2109/jcersj2.17162.
24. Oku, T. Crystal structures of perovskite halide compounds used for solar cells. *Rev. Adv. Mater. Sci.* **2020**, *59*, 264–305, doi:10.1515/rams-2020-0015.
25. Ueoka, N.; Oku, T.; Ohishi, Y.; Tanaka, H.; Suzuki, A. Effects of excess PbI_2 addition to $CH_3NH_3PbI_{3-x}Cl_x$ perovskite solar cells. *Chem. Lett.* **2018**, *47*, 528–531, doi:10.1246/cl.171214.
26. Oku, T.; Ohishi, Y.; Ueoka, N. Highly (100)-oriented $CH_3NH_3PbI_3$(Cl) perovskite solar cells prepared with NH_4Cl using an air blow method. *RSC Adv.* **2018**, *8*, 10389–10395, doi:10.1039/c7ra13582c.
27. Ueoka, N.; Oku, T.; Tanaka, H.; Suzuki, A.; Sakamoto, H.; Yamada, M.; Minami, S.; Miyauchi, S.; Tsukada, S. Effects of PbI_2 addition and TiO_2 electron transport layers for perovskite solar cells. *Jpn. J. Appl. Phys.* **2018**, 57, 08RE05, doi:10.7567/JJAP.57.08RE05.